buildings

MDPI

Article

Heat Transfer Behavior of Green Roof Systems under Fire Condition: A Numerical Study

Nataliia Gerzhova [1,*], Pierre Blanchet [1], Christian Dagenais [1,2], Jean Côté [3] and Sylvain Ménard [4]

1 NSERC Industrial Research Chair on Eco-responsible Wood Construction (CIRCERB), Department of Wood and Forest Sciences, Université Laval, Québec G1V 0A6, QC, Canada; Pierre.Blanchet@sbf.ulaval.ca (P.B.); Christian.Dagenais@fpinnovations.ca (C.D.)

2 FPInnovations, Québec G1V 4C7, QC, Canada

3 Department of Civil and Water Engineering, Université Laval, Québec G1V 0A6, QC, Canada; Jean.Cote@gci.ulaval.ca

4 Université du Québec à Chicoutimi (UCAQ), Chicoutimi G7H 2B1, QC, Canada; Sylvain_Menard@uqac.ca

* Correspondence: nataliia.gerzhova.1@ulaval.ca

Received: 15 August 2019; Accepted: 3 September 2019; Published: 19 September 2019

Abstract: Currently, green roof fire risks are not clearly defined. This is because the problem is still not well understood, which raises concerns. The possibility of plants catching fire, especially during drought periods, is one of the reasons for necessary protection measures. The potential fire hazard for roof decks covered with vegetation has not yet been fully explored. The present study analyzes the performance of green roofs in extreme heat conditions by simulating a heat transfer process through the assembly. The main objective of this study was to determine the conditions and time required for the roof deck to reach a critical temperature. The effects of growing medium layer thickness (between 3 and 10 cm), porosity (0.5 to 0.7), and heating intensity (50, 100, 150, and 200 kW/m^2) were examined. It was found that a green roof can protect a wooden roof deck from igniting with only 3 cm of soil coverage when exposed to severe heat fluxes for at least 25 minutes. The dependency of failure time on substrate thickness decreases with increasing heating load. It was also found that substrate porosity has a low impact on time to failure, and only at high heating loads.

Keywords: green roof; fire; heat transfer; modeling

1. Introduction

The current increase in the use of green roofs requires an assessment of the safety aspect, including their fire behavior. Even though these systems, as a modern technology, have existed for about 40 years, their fire performance is still debated. In an attempt to design safe green roofs, a large experimental research was conducted in Germany in the 1980s. Based on the results, the first fire protection measures were developed and made a part of the German green roof design guideline FLL [1]. There is an opinion that green roofs can protect a building from fire, and it was mentioned that, in the past, some green roofs were installed to resist fire propagation [2]. This belief is due to the fact that plants are about 95% of water. However, concerns arise in the case when a green roof has dried up, due to poor maintenance or during hot summer periods. Dried plants and accumulated debris may be easily ignited, and therefore, contribute to fire. This was demonstrated recently by a fire that occurred in the summer of 2018, in Portland [3], where a poorly maintained vegetated roof with overgrown plants caught fire from the sparking of a nearby transformer. Although the damages and losses were not substantial, this incident confirms the possibility of fire on green roofs.

To conform to building regulations, roof coverings are evaluated according to test standards CAN/ULC-S107 [4] in Canada or ASTM E108 [5] in the United States. The samples are tested for their

ability to resist the spread of flame and downward flame propagation through the deck (for combustible decking). Even though green roof manufacturers successfully tested their assemblies following these standards, it is still difficult to conduct the tests on such roofs, due to the specificity of the components. The conditions for testing the assembly are unclear, such as the presence of vegetation, level of compaction of the growing medium, moisture content of the growing medium and plant material, and associated difficulties. The absence of an established test procedure specifically for green roofs makes it difficult to correctly classify their fire performance.

In order to shed some light on the fire safety of green roofs, or factors affecting their fire performance, a necessity emerges to conduct research that will not repeat a standard test but show and analyze a green roof's response to fire in the most severe conditions. This would demonstrate the potential fire hazard that a green roof could pose to a building. For this particular study, a downward heat transfer was analyzed for predicting the possible damages to a roof deck caused by a fire on the roof. Decking materials, such as wood or steel, can be affected by a high temperature, which can lead to the structural failure. A downward heat transfer was chosen due to the risk of damage to a roof deck. This is because a green roof fire was identified as the main concern of some Authorities Having Jurisdiction.

There is limited data available from fire tests previously conducted on green roofs. Large-scale fire tests conducted according to DD CEN/TS 1187 "Test methods for external fire exposure to roofs" [6] (analogue to CAN/ULC-S107) in the UK aimed to determine the possibility of fire spreading into the building in the case where a roof surface was exposed to fire [7]. In the experiment (burning brand test), the specimen consisted of a growing medium layer of 8 cm thickness and no plants on top. It was shown that the temperature measured under the soil layer did not exceed 100 °C—which was insufficient to ignite the layers underneath, and thus, no fire penetration could occur. Similar burn-through tests were performed on green roof assemblies [8]. Specimens consisted of a 5 cm thick growing medium, a 2.5 cm thick drainage layer, and a 0.5 cm thick protection mat, thermal insulation, and steel deck. After the end of the test (which took approximately 30 min), a temperature of 40 °C was registered under the soil layer even though the soil surface reached 300 °C. The drainage and all other layers, thus, remained intact. Even though both tests showed that a substrate layer could protect from fire penetration, no detailed data was provided with respect to the effects of soil moisture level, composition, amount of organic matter (OM), or temperature evolution during the test. Moreover, it is unclear from these results whether the soil thickness is an important parameter that influences heat conduction. Given that a green roof is a multiple-layer assembly, with different characteristics of each component, it is important to understand which factors affect the most the heat transfer in the event of a fire.

Although there are well-accepted methods to carry out full-scale experimental investigations that evaluate possible damages due to fire, conducting tests is a complex, labor- and time-consuming process of creating conditions and specimen preparation. Instead, the heat transfer problem can be successfully solved by numerical simulations. This is a good alternative approach, provided the modeling is verified and validated by test data. This method allows for the analysis of different scenarios in a relatively simple and fast way.

The objective of this research is to assess the fire risk that a green roof can present to a roof structure using numerical simulation. Specifically, it aims to determine under which conditions the roof deck can be damaged if the green roof is exposed to elevated temperatures from the exterior. It also aims to determine which configuration of vegetated roof assemblies or characteristics of its components present a greater fire risk. Due to great variability in factors that affect weather conditions on a roof, some simplifications were made, such as for the heating load. The analysis was, thus focused on the simulations of the worst cases.

2. Methodology

2.1. Numerical Modeling

Numerical models were developed that could represent heat transfer through green roof assemblies of different geometries, with the purpose to analyze the temperature response of these roofing systems to extreme heat, and to determine at which conditions a system may fail. Specifically, they determine the moment at which the roof deck reaches its critical temperature (failure time). The model contains simplifications, such as the thermal load is constant for the whole duration of simulation, the condition that the heat transfer occurs by conduction only, and that no heat generation within a soil layer is considered. Although the thermal decomposition of the soil OM can contribute to heat propagation, its content in the substrate for green roofs is usually low, within 3–6% by mass, and thus, neglected.

The one-dimensional heat transfer is described by the following partial differential Equation (1):

$$\frac{\partial}{\partial x}\left(\lambda\frac{\partial T}{\partial x}\right) = \rho C_P\frac{\partial T}{\partial t}, \tag{1}$$

where λ, C_P and ρ are the thermal conductivity (W/(m·K)), specific heat (J/kg·K) and density (kg/m^3) of each material, respectively. x is the depth (m), T is temperature (K) and t is time (s). All material characteristics are temperature-dependent, as presented in the next section.

The initial temperature in the model is 22 °C (295 K). The boundary condition at the soil surface ($x = 0$) exposed to heat is a combination of convective and radiative heat fluxes:

$$q_1'' = q_{rad}'' + q_{conv}'' = h_1\left(T_f - T_s\right) + F\varepsilon\sigma\left(T_f^4 - T_s^4\right), \tag{2}$$

where q''_1 is the net heat flux, q''_{rad} is the radiative heat flux, q''_{conv} is the convective heat flux, h_1 is the convective heat transfer coefficient equal to 25 W/(m^2·K); T_f is the source temperature (K); T_S is the temperature of a receiving surface (K); F is the view factor assumed 1; ε is the emissivity assumed to be equal to 0.8; σ is the Stefan–Boltzmann constant equal to 5.67×10^{-8} W/(m^2·K^4). For the underside of the roof deck the heat loss is:

$$q_2'' = h_2(T_s - T_a), \tag{3}$$

where *Ta* is the ambient temperature set at 295 K, h_2 is the convective heat transfer coefficient equal to 9 W/(m^2·K), which, according to EN 1991-1-2 [9], can be assumed to contain the effect of heat transfer by radiation.

2.2. Modeling Parameters

2.2.1. Geometry

A typical green roof assembly consists of a soil layer, drainage, insulation (optional) and a roof deck. Other layers, such as filter sheet, root barrier and waterproof membrane are of small thicknesses and will most likely not greatly affect the temperature evolution in the assembly, therefore these components are not included in the numerical models. For green roofs one of the most common insulation materials is extruded polystyrene (XPS), lightweight rigid boards, resistant to water and with good compressive strength. However, XPS is a highly flammable material that softens, then rapidly melts and loses its structure as it reaches 100 °C, which can lead to changes in geometry of the assembly. Therefore, only geometries without insulation are used for the simulations. A granular material forming a 2 cm thick layer is used for the drainage. The description of the material is presented in the next sections. Two different types of roof deck susceptible to heat damage are selected for the modeling. A wooden deck made of plywood of 19 mm thickness and a corrugated steel deck (modeled as a flat steel sheet of 1.5 mm in thickness). In such cases, a gypsum board (Type X, 13 mm) is usually placed on top of the deck to provide fire protection due to the fire resistance properties of such boards.

It is also used as a cover board to ensure a flat surface, when installing vegetated roof over the steel deck. To analyze the most severe case, additionally, the assembly installed on a wood deck without gypsum board on top is used. Figure 1a,b and Figure 2 show the green roof assemblies used for the modeling.

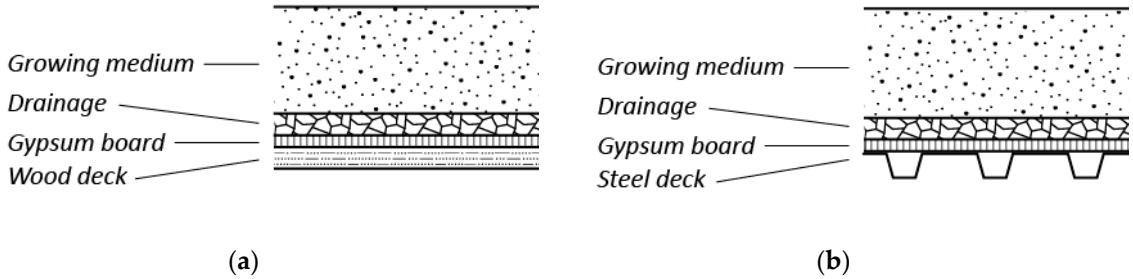

Figure 1. Assemblies with the gypsum board installed over a: (**a**) Wood deck; (**b**) steel deck.

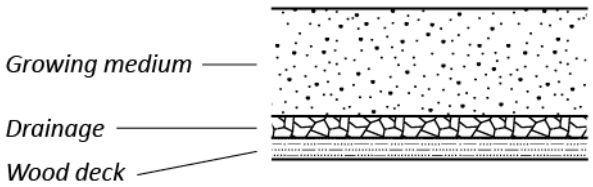

Figure 2. Assembly installed over a wood deck, without gypsum board.

Since the objective of the analysis is to identify under which conditions the roof deck can be damaged, the critical temperature for the decking material will be an indicator of roof failure. The critical condition for the plywood deck is a state at which charring is initiated. Thus, a charring temperature of 300 °C is chosen as critical, as per EN1995-1-2 (2003). For steel, a temperature of 538 °C (1000 °F) is considered a failure criterion according to the ASTM International fire resistance test for steel structures [10].

2.2.2. Growing Medium

Substrate thermal and physical properties are determining factors in heat conduction and therefore their impact needs to be examined. As this study focuses on the analysis of the most severe conditions, only dry soil is considered. Moisture causes a delay in temperature increase in soil at about 80–100 °C until almost all water vaporizes, whereas the temperature rise in dry soil is smoother at all depths and reaches higher values [11]. Temperature profiles of dry natural soils during fires have been experimentally studied in the past [12–15]. It was shown that dry soil is a poor thermal conductor and prevents the heat from propagating downwards, causing a large temperature gradient to appear. Measurements during wildfires showed that dry soil, reaching high temperatures at the surface, over 700 °C, stayed in the range of 43 to 54 °C at a depth of 5 cm [12]. Another study showed that the temperature at a depth of 1 cm increased to only 46 °C, while the surface reached 362 °C during a fire of low intensity [13]. Other studies have provided the following data: the temperature of soil during forest fires measured at the surface reached 450 °C, while it reached 45 °C on average at a depth of 5 cm [14]; a peak temperature of 700 °C at the surface and 440 °C at a depth of 2 cm in dry sand [15]. Therefore, the soil layer can greatly reduce the heat penetration down to the roof elements below. Similar behavior is expected from green roof growing medium, as it contains large amount of porous aggregate with low thermal conductivity. The minimum thickness of growing medium for green roofs in Canada is usually 10 cm [16,17]. However, German FLL guideline contains a description of a green roof that is considered resistant to radiant heat (hardroof) when substrate depth is at least 3 cm. Thus, several models need to be performed to determine the depths of the growing medium sufficient to resist the propagation of heat down to the roof deck. In view of the objective of this research to

model the response of green roof assembly to extreme heat in most severe cases, the smallest growing medium thickness required in Canada, 10 cm, was chosen for the simulations. Simulations of green roof assemblies with smaller thicknesses of growing medium were performed, namely with 3, 5 and 7.5 cm to investigate the effect of substrate thickness on time to failure of a roof structure.

Another factor affecting soil heat transfer performance is porosity. Growing media on green roofs can have different levels of compaction, which, among other factors, depend on the age of roof, since the soil naturally settles and becomes denser with time. This parameter directly affects thermal conductivity. In dry soil, heat is transmitted by conduction mainly through the solid particles because air, contained in pores, has a very low thermal conductivity. A smaller porosity means more solid particles per unit volume of soil and thermal conductivity therefore increases [18]. A typical growing medium was characterized in a previous work [19]. Maximum and minimum possible porosities of dry samples reached by manual compaction were 0.7 and 0.5.

2.3. Material Characteristics

2.3.1. Growing Medium

The heat transfer in granular materials such as soil is a complex process. Previous work on the prediction of the effective thermal conductivity (λe) of dry green roof substrate as a function of temperature has been conducted specifically for application in numerical simulations [19]. In the present study, λe was calculated for different temperatures using the same method and data, but for a growing medium containing 5% OM by mass, which is typical for extensive green roof systems. The effective thermal conductivity is a sum of the thermal conductivity of a dry substrate (λc) and the contribution of interparticle radiation (λrad):

$$\lambda_e = \lambda_c + \lambda_{rad}, \tag{4}$$

where λc is calculated with the Côté and Konrad model [20] as:

$$\lambda_c = \frac{\left(\kappa_{2P}\lambda_s - \lambda_f\right)(1-n) + \lambda_f}{1 + (\kappa_{2P} - 1)(1-n)}, \tag{5}$$

where λs and λ_f are the temperature dependent thermal conductivities of soil solids and air respectively in W/(m·K), n is the porosity, which is assumed constant, and κ_{2P} is a structure parameter. λ_f was taken from the literature [21]. λs as a function of temperature was taken from Gerzhova et al. [19] considering 5% OM and the loss of OM with increasing temperature according to the thermal decomposition curve shown in Figure 3.

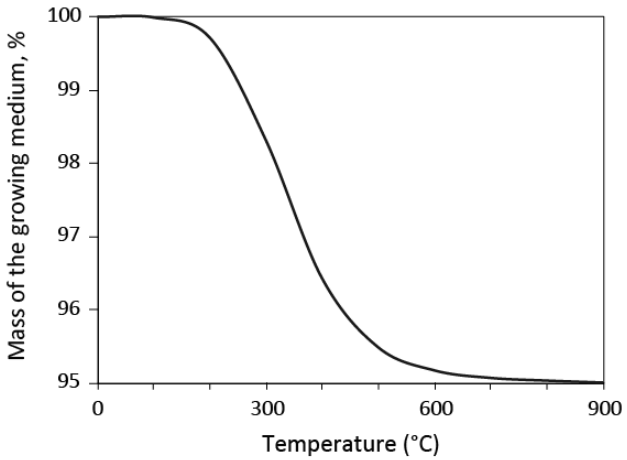

Figure 3. The loss of organic matter (OM) in the growing medium with respect to temperature.

The structure parameter was obtained with the equation of Côté and Konrad [20]:

$$\kappa_{2P} = 0.29\left(15\frac{\lambda_f}{\lambda_s}\right)^{\beta}, \quad (6)$$

where β was determined in the previous study for green roof soils and is equal to 0.3. The radiation contribution to λe was calculated as:

$$\lambda_{rad} = 4Ed_{10}\sigma T^3, \quad (7)$$

where E is the exchange factor equal to 0.82, d_{10} is the particle diameter equal to 2 mm (from the data provided by the manufacturer), σ is the Stefan–Boltzman constant equal to 5.67×10^{-8} (W/(m^2·K^4)), T is the temperature (K). Figure 4 shows the effective thermal conductivity of the growing medium that was used in the modeling.

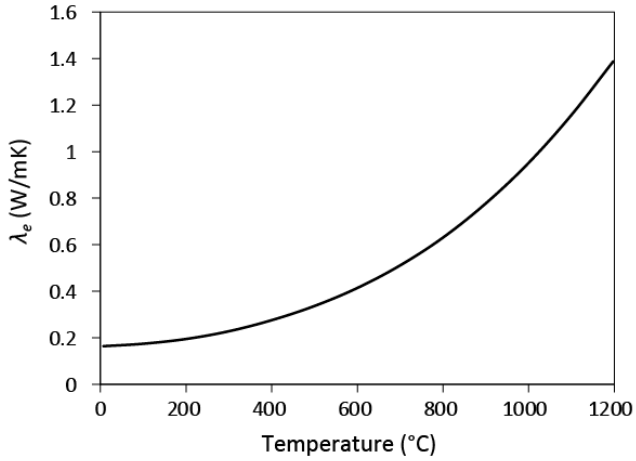

Figure 4. Effective thermal conductivity of the growing medium.

The density (ρ) was calculated using porosity (n) and the data on particle densities:

$$n = 1 - \frac{\rho}{\rho_{solid}}, \quad (8)$$

where n is the porosity, ρ is the bulk density (kg/m^3) and ρ_{solid} is the particle density (kg/m^3). The loss of OM, that has low ρ_{solid}, at high temperature leads to changes in proportion of the components of the substrate, and therefore, changes in the substrate mean particle density and bulk density. In the previous study on the same substrate, ρ_{solid} of its inorganic part was measured and was equal to 2470 kg/m^3. ρ_{solid} of the substrate with 5% OM is 2400 kg/m^3, which is obtained taking ρ_{solid} of OM equal to 1300 kg/m^3 [22]. It has been verified with a furnace test that the soil porosity of 0.6 remains the same before and after burning. For simplicity, it is assumed that other porosities used in the modeling do not change. Figure 5 shows temperature dependent densities for each porosity, which slightly increase after the loss of OM.

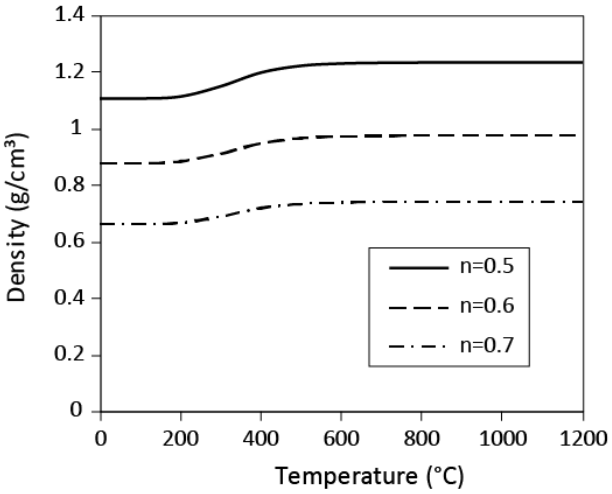

Figure 5. Temperature dependent densities of the growing medium according to porosities (*n*) 0.5, 0.6, and 0.7.

Specific heat at different temperatures was obtained as a sum of specific heat of mineral and organic parts multiplied by their mass fractions [22]:

$$C_P = \sum_{i=1}^{n} C_{P_i} x_i, \tag{9}$$

where C_P is the specific heat in J/(kg·K), x is the mass fraction, and i is the component. Specific heat of OM is kept constant and equal to 1925 J/(kg·K). The specific heat of the mineral component is, however, a temperature-dependent property and can be predicted with the equation proposed by Waples and Waples [23]:

$$C_{P_{T2}} = C_{P_{T1}} \cdot C_{Pn_{T2}} / C_{Pn_{T1}}, \tag{10}$$

where $C_{P_{T1}}$ is the specific heat at normal temperature equal to 770 J/(kg·K) [23]. C_{Pn_T} is the normalized specific heat capacity at a certain temperature (T) obtained with:

$$C_{Pn_T} = 8.95 \cdot 10^{-10} T^3 - 2.13 \cdot 10^{-6} T^2 + 0.00172T + 0.716, \tag{11}$$

Figure 6 is the resulting curve of the specific heat that was used for the simulation.

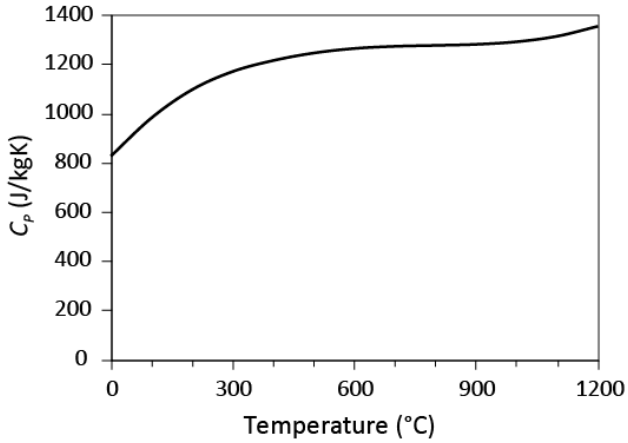

Figure 6. Specific heat of the growing medium at different temperatures.

A simplified validation test using a cone calorimeter apparatus was performed in the previous study on the thermal properties of the same green roof substrate [19]. It was concluded that the thermal properties used in the model are suitable for simulation purposes.

2.3.2. Other Components

It is considered that the drainage layer is made of a granular material, a porous lightweight aggregate that serves to drain water. Its thermal conductivity can be obtained by the same method as for the growing medium [Equations (4)–(6)]. As it is used as one of the components in the growing medium, several of its physical characteristics are known from the previous study [19]. The λs of the aggregate particles was measured and is equal to 0.82 W/(m·K). κ_{2P} is obtained by taking β equal to 0.54 for materials with angular shaped particles, according to Côté and Konrad [20]. Assuming λs is constant with temperature and n is equal to 0.5, λc can be determined with Equation (5). The radiation contribution to the thermal conductivity is similar to that of the growing medium since d_{10} is 2 mm (laboratory analysis provided by the manufacturer) and E is assumed to be 0.82. The effective thermal conductivity for a drainage layer is therefore obtained and presented in Figure 7.

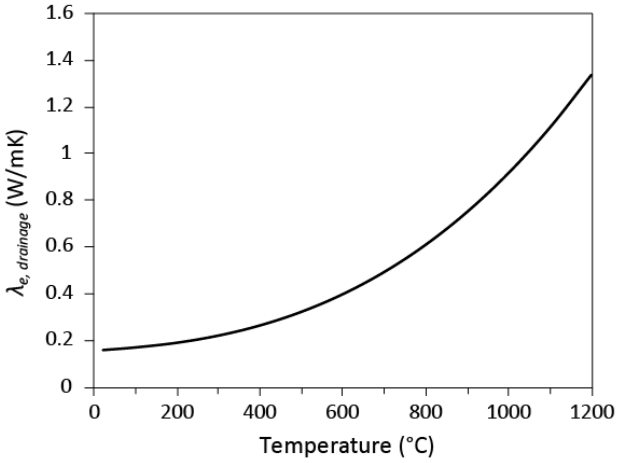

Figure 7. Effective thermal conductivity of the drainage layer.

The density of the drainage layer is 1050 kg/m^3, which is obtained from Equation (8) using the data on the measured particle density of 2100 kg/m^3 and assuming a porosity 0.5. It is noted that the material itself is steel slag. The specific heat of slag at different temperatures has been studied by Gil et al. [24]. The results of this research were used for the simulations and are presented in Figure 8.

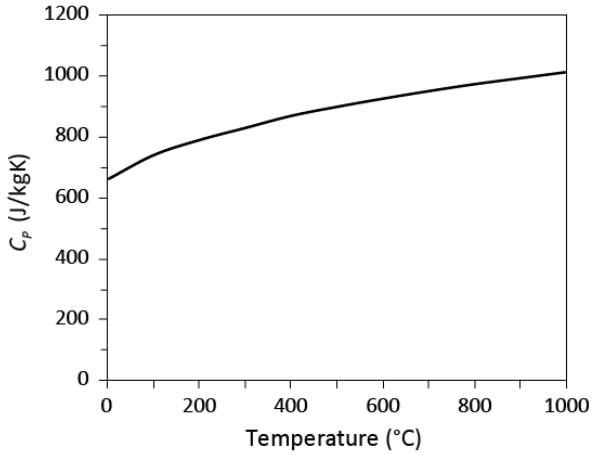

Figure 8. Specific heat of the drainage layer with respect to temperature.

The temperature dependent properties of other components in the assembly used in the numerical modeling are presented in the literature by standards and research documents. Properties for the wood are presented in Figure 9a–c [25]. Type X gypsum board properties are shown in Figure 10a–c [26] with the density equal to 836.4 kg/m^3 at 20 °C [27].

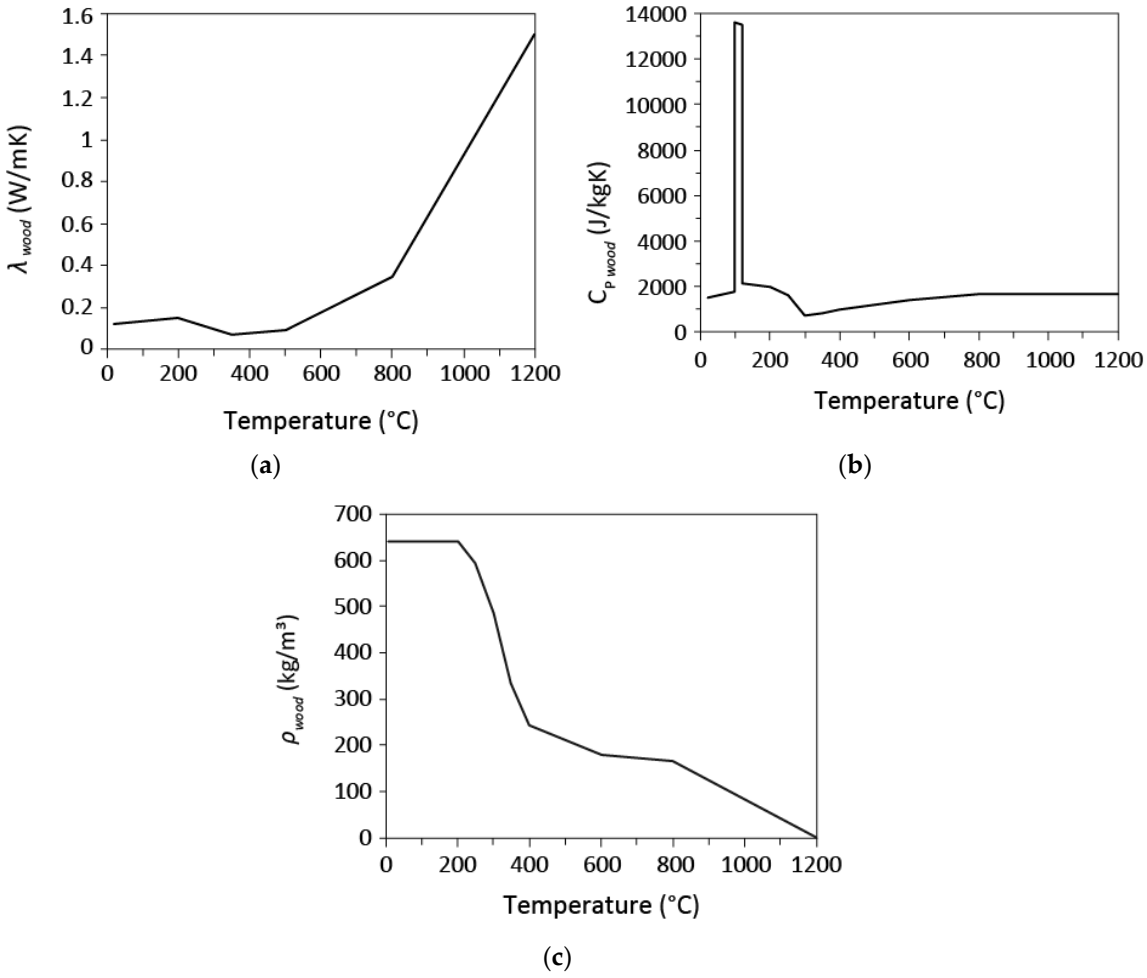

Figure 9. Temperature dependent properties of wood: (**a**) Thermal conductivity; (**b**) specific heat; (**c**) density.

Steel density is kept constant and is equal to 7850 kg/m^3. Thermal conductivity of steel as a function of temperature can be obtained with Equation (12) for a temperature range between 20 and 800 °C, keeping a constant value of 27.3 W/(m·K) above 800 °C [28].

$$\lambda_{steel} = 54 - 3.33 \cdot 10^{-2} T \quad (12)$$

where T is the temperature (°C). The specific heat for steel is calculated with Equation (13.1) (for T between 20 and 600 °C), Equation (13.2) (for T between 600 and 735 °C) and Equation (13.3) (for T between 735 and 900 °C). For a temperature range between 900 and 1200 °C, the specific heat of steel is equal to 650 J/(kg·K) [28].

$$C_{P,\,steel} = 425 + 7.73 \cdot 10^{-1} T - 1.69 \cdot 10^{-3} T^2 + 2.22 \cdot 10^{-6} T^3 \quad (13.1)$$

$$C_{P,\,steel} = 666 + 13002/(738 - T) \quad (13.2)$$

$$C_{P,\,steel} = 545 + 17820/(T - 731) \quad (13.3)$$

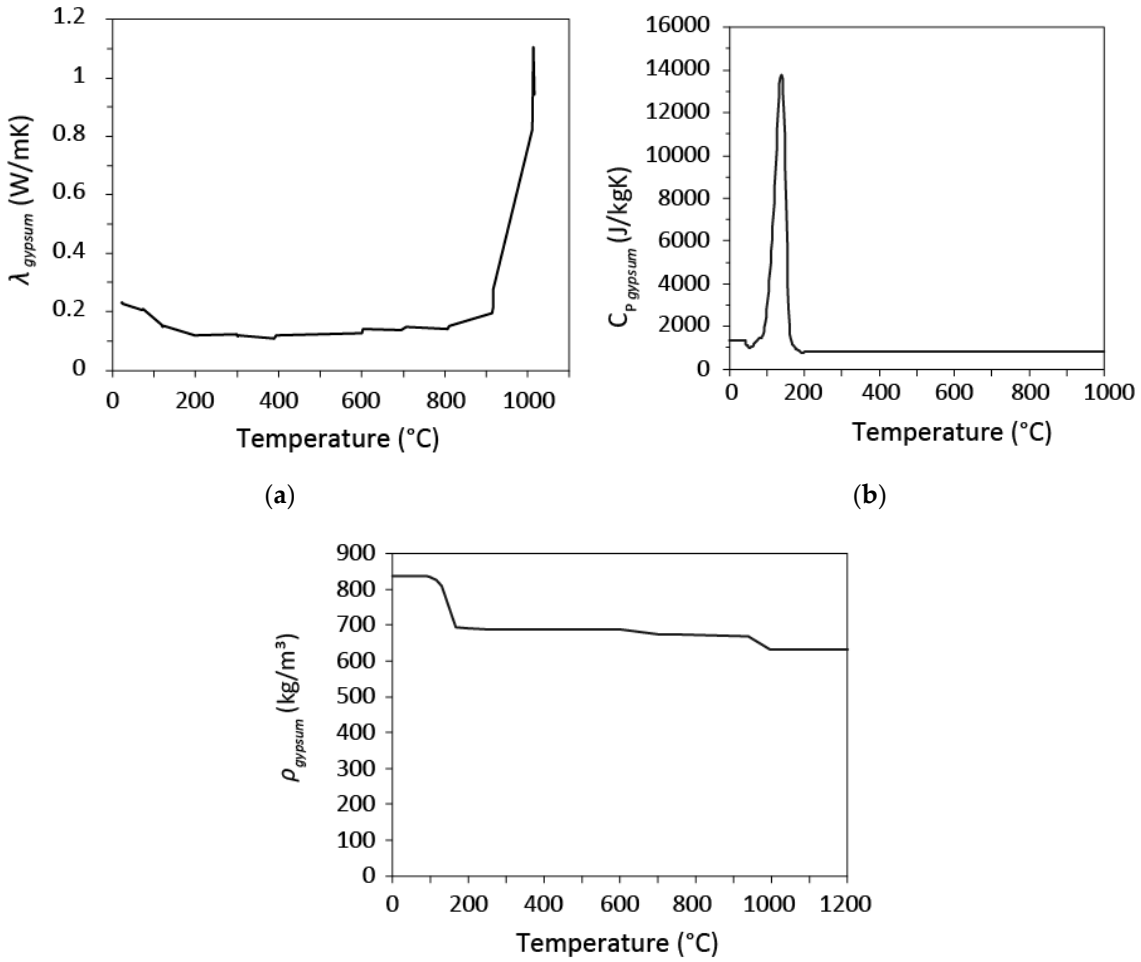

Figure 10. Temperature dependent properties of type X gypsum board: (**a**) Thermal conductivity; (**b**) specific heat; (**c**) density.

2.4. Thermal Load

The thermal response of a structure is largely dependent on the heating load applied, or fire intensity. In the research on fire spread in wildlands, a peak radiant heat flux of 51 kW/m^2 was registered ahead of the fire front and suggested as a representative value in wildfires [29]. Larger heat fluxes of up to 200 kW/m^2 were measured in forest fires [30]. Four thermal loads were used in the modeling: 50, 100, 150 and 200 kW/m^2 for a duration of four hours. In order to describe the thermal loads, a correspondence of heat flux to a temperature is shown using a time-temperature curve of a standard fire resistance test CAN/ULC-S101 [31]. The dashed line in Figure 11 shows the evolution of temperature with time in the furnace during the standard CAN/ULC S101 test.

The heat flux curve (solid line) was obtained with Equation (2) and is the sum of the radiative and convective heat fluxes. The correspondence to temperature (T_f) was determined by taking the convective heat transfer coefficient (h_1) equal to 25 W/(m^2·K), the configuration factor (F) equal to 1 and the emissivity (ε) equal to 0.8. Table 1 contains the heat flux characterization, where, for example, a heat load of 200 kW/m^2 corresponds to a 240 min standard fire-resistance test, time at which the temperature inside the furnace is 1110 °C. This relationship also corresponds to the measured values from Sultan [32].

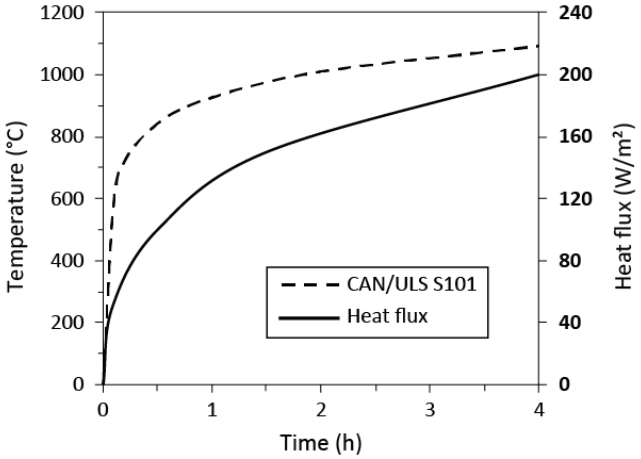

Figure 11. CAN/ULC S101 standard fire curve and corresponding heat flux.

Table 1. Heat flux characterization.

Load (Heat flux)	Temperature	CAN/ULC S101 Time
kW/m^3	**°C**	**Minutes**
50	623	7
100	850	33
150	1000	112
200	1110	240

After performing several preliminary simulations, a time step of 20 seconds was elected for all simulations. The mesh for the assemblies with a wooden deck was composed of linear elements of 5 mm each for the soil and the drainage layer, and four elements for a wooden deck. For the assembly that contains gypsum board and a metal support, the mesh included equal elements of 5 mm for the soil and the drainage layers, six elements for the gypsum board and one element for the steel deck. The sensitivity test was performed for a mesh size of the substrate and drainage layers. The results of simulations with 2 mm elements showed the difference in temperature profiles of less than 1 °C. The elements of these layers were set to 5 mm for all simulations to reduce calculation time. The transient heat transfer calculations were performed in ANSYS Mechanical (version 18.2), finite element analysis software.

3. Results and Discussion

3.1. Temperature Profiles

Several models were performed to simulate the response of green roof assemblies to fire. Figure 12a,b and Figure 13 show temperature profiles for the different assemblies with a 10 cm thick growing medium and a porosity of 0.6 during exposure to a heat load of 50 kW/m^2 for four hours. It can be seen that the heat slowly penetrated the growing medium layer, creating a smooth temperature gradient, especially after a long period of heating. The temperature below the growing media started to rise after 40 minutes and at a very slow rate. No temperature increase was observed at the roof deck after the first hour. Further, these layers were still not affected after the second hour of exposure, not exceeding a temperature of 50 °C. In all cases, the critical temperature at the deck was not reached during the 4 h heating period. The temperature at the top of the wooden deck not covered by a gypsum board reached only 110 °C, and 178 °C under the substrate (10 cm depth) (Figure 13). In the case of the presence of a Type X gypsum board, the wooden deck reached only 86 °C, while the metal deck temperature was only slightly increased to 69 °C (Figure 12). The temperatures at a 10 cm depth were comparable to values given in the literature for temperature profiles of soils during forest

fires. For example, after two hours the temperature reached 79 °C (Figure 12b) and 73 °C (Figure 13). In the research by Busse et al. [33] about 80 °C was registered in dry mineral soil (ρ = 1000 kg/m^3) at a 10 cm depth after two hours of fire. However, the heat load at the surface decreased with time, which led to smaller values at durations of more than two hours. Campbell et al. [34] recorded about 260 °C at a depth of 3.6 cm in dried natural soil during exposure to a heat flux between 39 and 54 kW/m^2. A temperature of 270 °C at the same depth and for the same heating time was found in the present study.

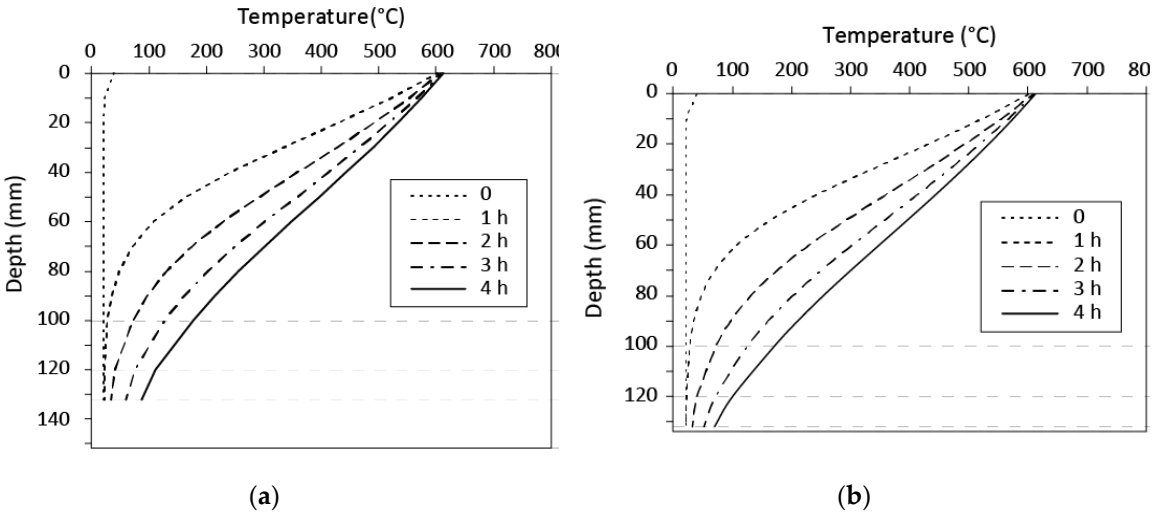

Figure 12. Temperature distribution in green roof assemblies: (**a**) With wooden deck; (**b**) with steel deck.

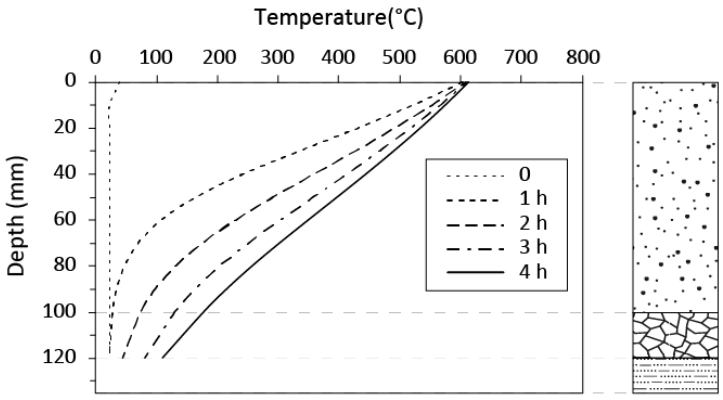

Figure 13. Temperature distribution in a green roof assembly installed over a wood deck and without gypsum board.

While exposed to a heat load of such intensity, the roof structure remained intact when covered by a 10 cm thick dry growing media of medium porosity. An increased duration of heating caused a temperature rise at the depths of interest. However, the critical temperature under these conditions will not probably be reached in all assemblies since the temperature profile curves are almost linear after four hours of exposure (Figure 12a,b and Figure 13), which indicates the approaching of a steady state. Therefore, increasing the exposure time at such a heat load for more than four hours is not reasonable.

3.2. Thermal Load Effect

While a low heating load does not greatly affect the deck temperature and roof failure does not occur even after four hours, the increase of the imposed heat flux at the surface can influence the evolution of temperatures in the assembly. This is shown in Figure 14, where the green roof assembly

without gypsum board was subjected to heating loads of different intensities. The temperature underneath a substrate layer remained almost the same after one hour of exposure to higher thermal loads (Figure 14a). However, the difference was noticeable after two hours. The temperature increased almost twice when the thermal load was twice as high—124 °C with a heat load of 100 kW/m^2, and 73 °C when applying 50 kW/m^2. When applying 200 kW/m^2 the temperature was more than three times higher than when applying 50 kW/m^2, 256 °C compared to 73 °C. It was the same for temperatures at the top of the deck (Figure 14b). After two hours, the deck was at 43 °C under 50 kW/m^2, while under 200 kW/m^2 it reached 115 °C. The critical temperature was attained after 3 h 13 min, which is 45 min earlier than when exposed to 150 kW/m^2. Smaller heat loads did not lead to a failure under such conditions.

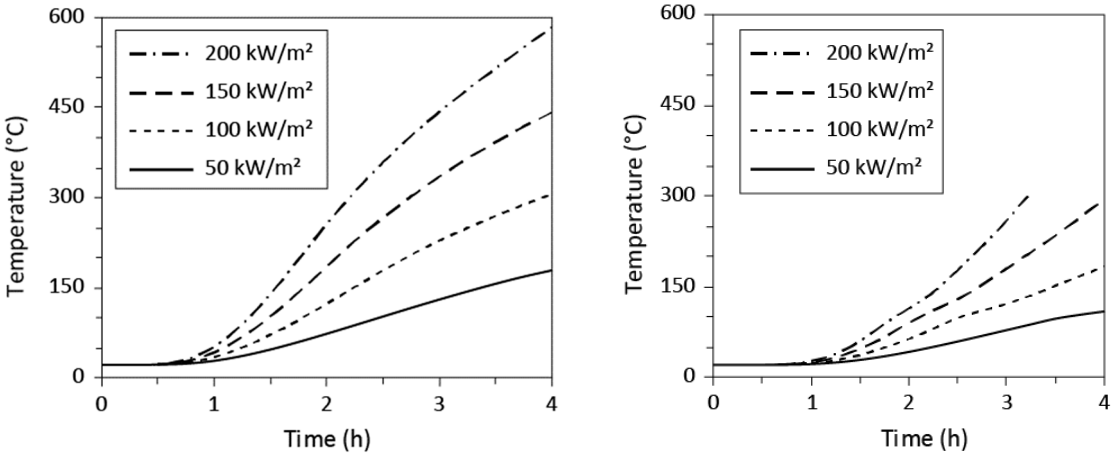

Figure 14. (**a**) Temperature evolution at the depth of 10 cm of a substrate layer within the green roof assembly installed on a wooden deck with no gypsum board; (**b**) temperature evolution at the top of the wooden deck.

Thus, the results suggest that the effect of thermal load is significant under such conditions, even though the growing media has low conductive characteristics and the layer is thick enough. The roof structure made of wood and not protected by a gypsum board (most severe case) is subject to a risk of failure only when the heating load is above 150 kW/m^2 for a period of four hours.

3.3. Substrate Thickness

The above analysis suggests that a 10 cm layer of growing medium insulates the roof by retarding the propagation of heat for at least three hours when exposed to a severe heat load. However, a thinner layer, may not be as effective at protecting the deck from heat damage. Critical temperatures reached at different soil thicknesses and applied thermal loads are presented in Figures 15 and 16 for the assemblies installed over the wooden deck with and without gypsum board, respectively. The curves represent the critical temperature reached by the deck at a certain thermal load.

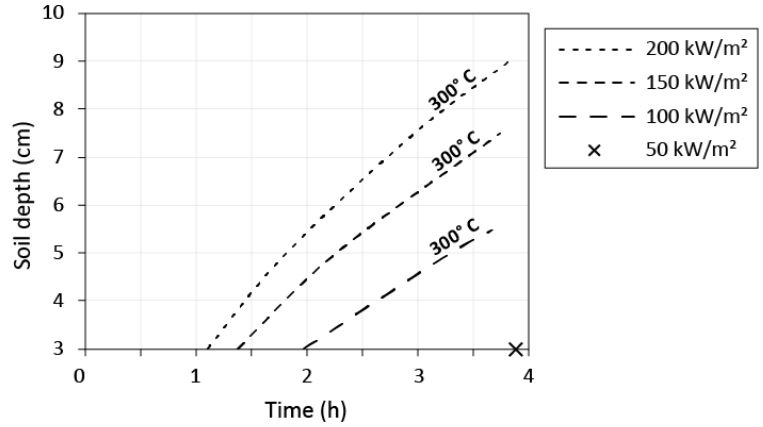

Figure 15. Assembly installed over a wooden deck with gypsum board. Relationship of time to failure of the deck (300 °C was reached under different thermal loads) and substrate thickness.

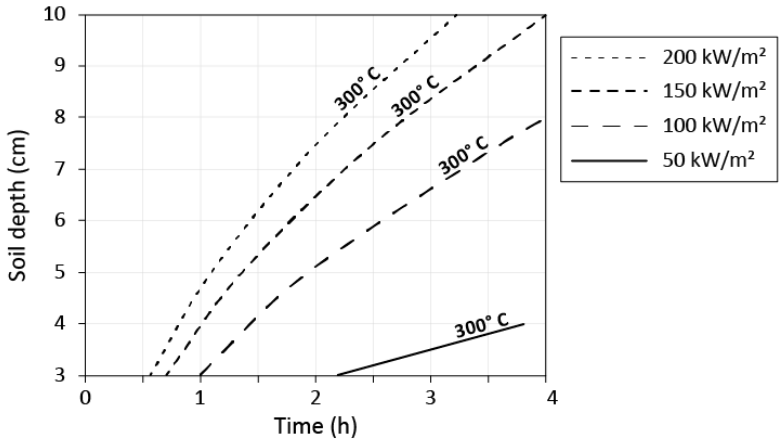

Figure 16. Assembly installed over a wooden deck without gypsum board. Relationship of time to failure of the deck (300 °C was reached under different thermal loads) and substrate thickness.

As expected, critical temperature was reached earlier as the thickness of soil decreases. When comparing the applied thermal loads, it was seen that in all cases the time to failure increases greatly for every additional cm of soil, especially for thermal loads of low intensity. For example, when imposing 100 kW/m^2, a deck, covered by a 5.5 cm soil layer and a gypsum board, reached 300 °C after 3 h 40 min, which is 1 h 40 min later when compared to the same assembly but with 3 cm of soil. A similar situation was observed for the assembly without gypsum. Under the same heat flux, the deck reached 300 °C at 2 h 15 min when protected with 5.5 cm of soil, while removing 2.5 cm led to much earlier failure, i.e., after one hour. At the same time, results show that with increasing thermal load the curves become steeper, which means lesser influence on dependence of time to failure on soil thickness. For instance, under 150 kW/m^2 the difference in failure time was 1 h 30 min when comparing assemblies with 7.5 and 5 cm thicknesses of growing media (Figure 15). A greater increase in heating intensity to 200 kW/m^2 for such thicknesses resulted in a smaller difference in time to failure, namely 1 h 10 min. For the assembly without gypsum board, the dependency of time to failure of the roof deck on thermal load intensity was less pronounced. Again, comparing soil coverages of 7.5 and 5 cm, the difference in the effect was 70 and 55 min, for 150 and 200 kW/m^2 respectively (Figure 16).

Considering the effectiveness of the growing media layer in protecting the roof from fire damage, it can be seen that, with decreasing thickness, the influence of heat load intensity on the time to roof failure becomes significantly smaller. Figure 15 shows that for the assembly with a 3 cm thick soil cover, the deck reached its critical temperature between 1 h 5 min and 2 h when exposed to thermal loads between 200 and 100 kW/m^2. Whereas, for the assembly with 5.5 cm of soil the critical temperature is

reached between 2 h and 3 h 40 min for the same thermal exposure range. This effect is more evident for the assembly with no gypsum board (Figure 16). Comparing applied thermal loads of 100 and 200 kW/m^2, in the assembly with 3 cm of soil, the deck reached the critical temperature after 60 and 35 min respectively, which is a 25 min time difference. Whereas in case of 8 cm of soil, the difference in failure time is 1 h 45 min, with failure occurring after 4 h and 2 h 15 min respectively for each thermal load.

When comparing the two assemblies with the wood deck it can be seen that the presence of gypsum board helps to greatly increase failure time, especially under low thermal loads. For example, the delay is one hour when applying 200 kW/m^2 for the roof with a 7.5 cm soil layer. For a smaller load of 150 kW/m^2, the delay is 1 h 15 min for the same assembly. Gypsum delays the deck failure in the assembly with the thinnest soil layer by 32 minutes for the maximum thermal load applied in the model and by 1 h 40 min for the minimum thermal load applied.

Failure is not expected, even with the shallowest growing media and under maximum thermal load, for the assembly with a steel deck. Figure 17 shows the roof deck temperature development where each curve represents the assembly with different soil layer thicknesses exposed to 200 kW/m^2. The better performance of such assembly in terms of time to failure compared to the assembly installed over a wooden deck is due to the higher critical temperature of steel. For example, the wood deck protected with gypsum board and 10 cm of soil reached a temperature of 235 °C after 4 h at 200 kW/m^2 while the steel deck reached 202 °C. Similar shape curves were obtained for all substrate layer thicknesses. It can also be seen that, at certain points, the 3 and 5 cm thickness curves show a slowing down of the temperature increase. The same model run for the assembly with 3 cm of soil and a 6 h duration does not show a significant increase in deck temperatures between 4 and 6 h of exposure to heat (results not shown). The reason is the approaching to reach steady state, as (not presented in the figure) the temperature under the substrate also slows to increase after about 2.5 h reaching 970 °C.

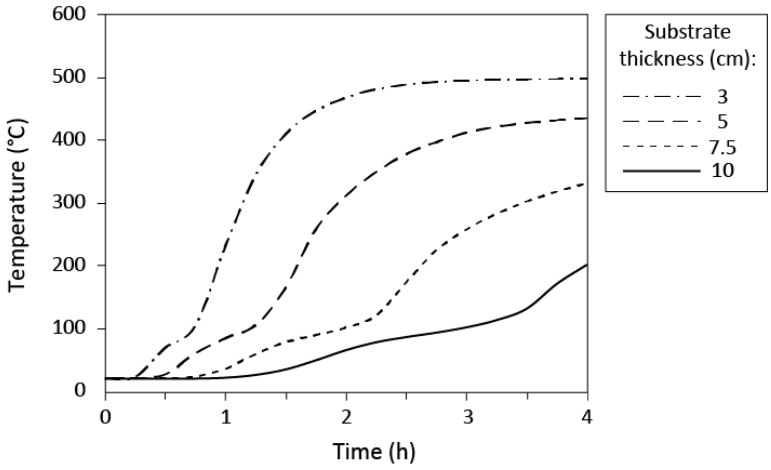

Figure 17. Temperature evolution at the deck (steel) level in the assembly exposed to 200 kW/m^2.

3.4. Substrate Porosity

Soil compacted to different porosities does not show great differences in reaching critical temperatures. Figure 18a,b shows the results of the deck temperature evolution with a 7.5 cm substrate layer and exposed to a heat load of 200 kW/m^2.

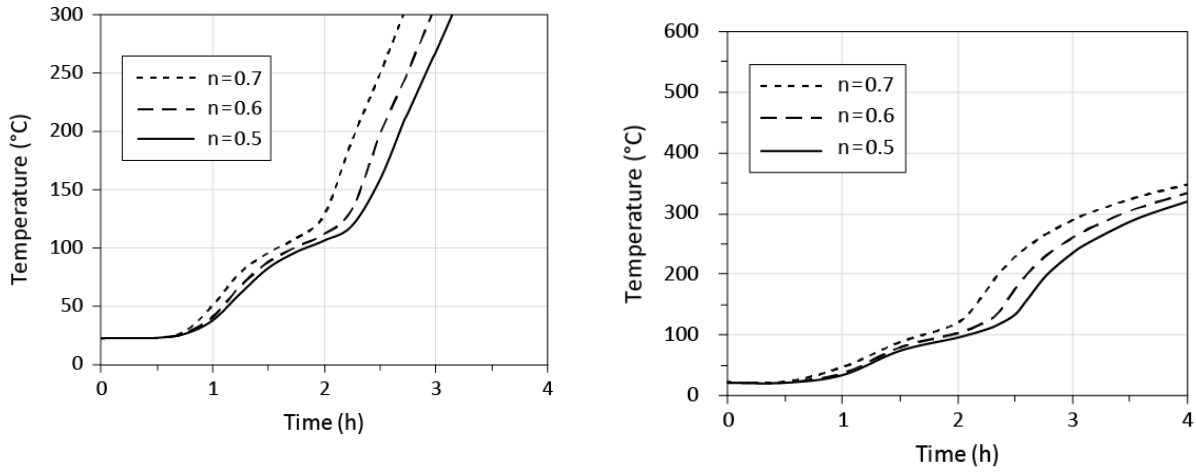

(**a**) (**b**)

Figure 18. Temperature evolution at the top of a deck with a 7.5 cm growing medium layer at three different porosities (*n*): 0.5, 0.6, and 0.7 when exposed to 200 kW/m^2; (**a**) wooden deck; (**b**) steel deck.

The smallest porosity of 0.5 (better compacted soil) retards the time to failure for the wood deck by 25 minutes compared to the assembly with a substrate porosity of 0.7, i.e., 3 h 9 min compared to 2 h 43 min (Figure 18a). For the assembly with the steel deck it can be seen that the porosity is not an important factor in roof failure because the critical temperatures are never reached, even at the shallowest soil layer (Figure 18b). Nevertheless, substrate shows the same behavior. Higher porosity leads to faster heating. For example, substrate of 0.7 porosity reached 100 °C 20 min earlier than the substrate of 0.5 porosity. The difference increases to 30 min when reaching 300 °C. The difference is smaller to insignificant at heating loads of lower intensity. When imposing 50 kW/m^2 temperature curves of the roof deck differ only by a few degrees (not shown).

Generally, soil compaction in green roof assembly determines, to some extent, heat propagation, especially in the case of severe fires, but not greatly.

4. Conclusions

This research explored the behavior of green roof systems when exposed to fire through the use of numerical modeling. A heat transfer analysis through the roof assembly was performed to predict the time to failure of a roofing deck in most severe fire cases. Only systems with a shallow growing media in completely dry conditions were examined.

Green roof substrate, sufficiently different from natural soils by composition and more bulky structure, still is comparable with some literature data for dry natural soils in temperature distribution along the depth when exposing to extreme temperatures. Due to its insulation characteristics, other layers in the assembly and a roof deck appeared to be effectively protected from damages by heat.

Near linear relationships were obtained between growing media thickness and time to failure of the roof when exposed to different heat fluxes. Greater substrate layer thicknesses delayed heat penetration through the assemblies. Also, an increased heat load had a smaller influence on the relationship between soil thickness and time to failure.

Assembly installed on a metal roof deck showed better performances in fire in terms of time to failure, namely due to a higher critical temperature of steel (538 °C) when compared to that of wood (300 °C).

Gypsum board greatly improved the performance of green roof installed over a wooden deck in fire by increasing the time to reach critical temperature for the whole range of heat load intensities.

A delay in reaching the critical temperature by the deck of at least 30 min can be attained in the roof assembly having at least 3 cm of substrate when exposed to intensive thermal load.

Substrate porosity had a small effect on the time to failure and only at high heat loads, which means that matured green roofs with settled growing media can have a slightly better performance under fire conditions than newly installed.

The present study examined green roof temperature responses to fire under idealized conditions. The scenarios studied are improbable since maintaining such high heat fluxes for a long period of time is not reasonable when taking into account only the vegetation as a fire load. Nevertheless, such an approach permitted the generalization of the behavior of such roofs during extreme heating. It was shown that the thicker the soil layer the better protection it provides for the roof deck when exposed to a heating load of any intensity, considered in this study, and at different compaction levels.

The limitation of these models is using the worst-case scenario in order to investigate conditions at which a structure failure is reached. Such idealizations can lead to overestimations of some results compared to real fires. Analyzing heat transfer in the assembly while taking into consideration several factors reflecting real fire conditions can be a subject for future research. These factors include boundary conditions on top, because the heat load is not uniform in its intensity in real fires and lasts for a shorter period. Another factor is the heat generation produced by OM combustion. Even though the amount of this material is small to negligible, including this portion of heat can improve the accuracy of the model. This can pose a challenge, as, in addition to collecting necessary information, understanding that incomplete combustion occurs at a certain depth due to a restriction of air access, adequate adjustments must be made. Developing a model that includes moisture in the growing medium would more realistically describe the fire performance of green roofs. The main effort in such model should be paid to the effect of water evaporation on the temperature development inside the assembly.

Another limitation is the lack of validation tests for the results due to the complexity in conducting such experiments. This is because of the absence of a standard method and equipment for providing 1D conduction that ensures the large scale application of controlled uniform heat loads downwards. A small-scale fire test in previous study [19] was conducted with a separate substrate layer to validate the heat transfer model and to verify the applicability of the thermal conductivity of a substrate determined in the study. Special arrangements and sample preparation were made to create modeled conditions as accurately as possible. Based on the satisfying test results of a previous research, simplified models were developed in this study with assemblies of green roof containing similar substrate and typical materials (structure, gypsum) with known properties.

Nevertheless, an intermediate-scale fire testing protocol should be developed to assess the fire behavior of realistic green roof assemblies, namely as it relates to heat transfer through the assembly based on similar failure criteria to those presented here. As an example, for a one hour fire resistance rated roof assembly, the time to reach its critical temperature should not be reached before one hour.

Author Contributions: Conceptualization, N.G. and P.B.; methodology, N.G., J.C. and C.D.; software, C.D.; validation, C.D., N.G. and J.C.; investigation, N.G.; resources, C.D.; writing—original draft preparation, N.G.; writing—review and editing, N.G., C.D, P.B. and S.M.; visualization, N.G.; supervision, P.B., C.D. and S.M.; funding acquisition, P.B.

Funding: The authors are grateful to Natural Sciences and Engineering Research Council of Canada for the financial support through its IRC and CRD programs (IRCPJ 461745-18 and RDCPJ 524504-18) as well as the industrial partners of the NSERC industrial chair on eco-responsible wood construction (CIRCERB).

Acknowledgments: Authors also acknowledge the Green Roof Working Group of the Green Building Council of Canada, Quebec's section for technical data and mobility funding.

Conflicts of Interest: The authors declare no conflict of interest.

References

1. FLL. *Guidelines for the Planning, Construction and Maintenance of Green Roofing—Green Roofing Guideline*; Preface: Bonn, Germany, 2008.

2. Köhler, M.; Schmidt, M.; Wilhelm, G.F.; Laar, M.; Paiva, V.L.D.; Tavares, S. Green roofs in temperate climates and in the hot-humid tropics–far beyond the aesthetics. *Environ. Manag. Health* **2002**, *13*, 382–391. [CrossRef]
3. Portland Fire Bureau. *Incident Report RP180057217*; Portland Fire Bureau: Portland, OR, USA, 2018.
4. ULC. *Standard Methods of Fire Tests of Roof Coverings*; CAN/ULC-S107; Underwriters Laboratories of Canada: Ottawa, ON, Canada, 2010.
5. ASTM International. *Standard Test Methods for Fire Tests of Roof Coverings*; ASTM E108-11; ASTM International: West Conshohocken, PA, USA, 2017.
6. CEN. *Test Methods for External Fire Exposure to Roofs*; DD CEN/TS 1187; CEN: London, UK, 2012.
7. Department for Communities and Local Government UK. *Fire Performance of Green Roofs and Walls*; Department for Communities and Local Government UK: London, UK, 2013; pp. 31–36.
8. Appl, R. New Fire Protection Tests on Green Roofs [ZinCo press release]. Available online: http://www.zinco.se/news/press_releases/press_release_details.php?id=64 (accessed on 18 November 2011).
9. European Committee for Standardization. *Eurocode 1: Actions on Structures-Part 1-2: General Actions-Actions on Structures Exposed to Fire*; EN 1991-1-2; European Committee for Standardization: Brussels, Belgium, 2003.
10. ASTM International. *Standard Test Methods for Fire Tests of Building Construction and Materials*; ASTM E119-12-a; ASTM International: West Conshohocken, PA, USA, 2012.
11. DeBano, L.F.; Neary, D.G.; Ffolliott, P.F. Combustion processes and heat transfer. In *Fire Effects on Ecosystems*; John Wiley & Sons: Hoboken, NJ, USA, 1998; pp. 19–45.
12. DeBano, L.F.; Rice, R.M.; Eugene, C.C. *Soil Heating in Chaparral Fires: Effects on Soil Properties, Plant Nutrients, Erosion, and Runoff*; Research Paper PSW-RP-145; Department of Agriculture, Forest Service, Pacific Southwest Forest and Range Experiment Station: Berkeley, CA, USA, 1979; p. 21.
13. Valette, J.C.; Gomendy, V.; Maréchal, J.; Houssard, C.; Gillon, D. Heat-transfer in the soil during very low-intensity experimental fires-the role of duff and soil-moisture content. *Int. J. Wildland Fire* **1994**, *4*, 225–237. [CrossRef]
14. Raison, R.J.; Woods, P.V.; Jakobsen, B.F.; Bary, G.A.V. Soil temperatures during and following low-intensity prescribed burning in a Eucalyptus pauciflora forest. *Aust. J. Soil Res.* **1986**, *24*, 33–47. [CrossRef]
15. Frandsen, W.H.; Ryan, K.C. Soil moisture reduces belowground heat flux and soil temperatures under a burning fuel pile. *Can. J. For. Res.* **1986**, *16*, 244–248. [CrossRef]
16. City of Toronto, Municipal Code, Chapter 492-9. *Toronto Green Roof Construction Standard: mandatory provisions*, 9 November 2017.
17. RBQ. *Critères Techniques Visant la construction de toits Végétalisés Quebec*; RBQ: Montréal, QC, Canada, 2015; pp. 15–16.
18. Farouki, O.T. *Thermal Properties of Soils*; U.S. Army Cold Regions Research and Engineering Laboratory: Hanover, NH, USA, 1981; pp. 12–29.
19. Gerzhova, N.; Côté, J.; Blanchet, P.; Dagenais, C.; Ménard, S. A conceptual framework for modelling the thermal conductivity of dry green roof substrates. *BioResour. J.* **2019**, *14*, 8573–8599.
20. Côté, J.; Konrad, J.M. Assessment of structure effects on the thermal conductivity of two-phase porous geomaterials. *Int. J. Heat Mass Transf.* **2009**, *52*, 796–804. [CrossRef]
21. Incropera, F.P.; Dewitt, D.P. *Fundamentals of Heat and Mass Transfer*; Wiley: Hoboken, NJ, USA, 2007; p. A-5.
22. De Vries, D.; Van Wijk, W. The Physics of plant environment. In *Environmental Control of Plant Growth*; Academic Press: Cambridge, MA, USA, 1963; pp. 5–22.
23. Waples, D.W.; Waples, J.S. A review and evaluation of specific heat capacities of rocks, minerals, and subsurface fluids. *Part 1: Minerals and nonporous rocks. Nat. Resour. Res.* **2004**, *13*, 97–122.
24. Gil, A.; Nicolas, C.; Ortega, I.; Risueño, E.; Faik, A.; Blanco, P.; Rodrıguez-Aseguinolaza, J. Characterization of a by-product from steel industry applied to thermal energy storage in Concentrated Solar Power. In *Proceedings of the 99th Eurotherm Seminar, Lleida, Spain*; Paper No. EUROTHERM99-01-066; 2014.
25. European Committee for Standardization. *Eurocode 5: Design of Timber Structures-Part 1-2: General-Structural Fire Design*; EN 1995-1-2; European Committee for Standardization: Brussels, Belgium, 2003.
26. Benichou, N.; Sultan, M.A.; MacCallum, C.; Hum, J.K. *Thermal Properties of Wood, Gypsum and Insulation at Elevated Temperatures (IR-710)*; National Research Council Canada: Ottawa, ON, Canada, 2001.
27. Ang, C.N.; Wang, Y.C. Effect of moisture transfer on specific heat of gypsum plasterboard at high temperatures. *Constr. Build. Mater.* **2009**, *23*, 675–686. [CrossRef]

28. European Committee for Standardization. *Eurocode 3: Design of Steel Structures-Part 1-2: Genera-Structural Fire Design*; EN 1993-1-2; European Committee for Standardization: Brussels, Belgium, 2005.
29. Silvani, X.; Morandini, F. Fire spread experiments in the field: Temperature and heat fluxes measurements. *Fire Saf. J.* **2004**, *44*, 279–285. [CrossRef]
30. Butler, B.W.; Cohen, J.; Latham, D.J.; Schuette, R.D.; Sopko, P.; Shannon, K.S.; Jimenez, D.; Bradshaw, L.S. Measurements of radiant emissive power and temperatures in crown fires. *Can. J. For. Res.* **2004**, *34*, 1577–1587. [CrossRef]
31. ULC. *Standard Methods of Fire Endurance Tests of Building Construction and Materials*; CAN/ULC-S101; Underwriters Laboratories of Canada: Ottawa, ON, Canada, 2014.
32. Sultan, M.A. Incident heat flux measurements in floor and wall furnaces of different sizes. *Fire Mater.* **2006**, *30*, 383–396. [CrossRef]
33. Busse, M.D.; Hubbert, K.R.; Fiddler, G.O.; Shestak, C.J.; Powers, R.F. Lethal soil temperatures during burning of masticated forest residues. *Int. J. Wildland Fire* **2005**, *14*, 267–276. [CrossRef]
34. Campbell, G.S.; Jungbauer, J., Jr.; Bristow, K.L.; Hungerford, R.D. Soil temperature and water content beneath a surface fire. *Soil Sci.* **1995**, *159*, 363–374. [CrossRef]